Crystallization Behavior and Mechanical Properties of Regiodefective, Highly Stereoregular Isotactic Polypropylene: Effect of Regiodefects versus Stereodefects and Influence of the Molecular Mass

Claudio De Rosa,*,† Finizia Auriemma,† Marcello Paolillo,† Luigi Resconi,‡ and Isabella Camurati‡

Dipartimento di Chimica, Università di Napoli "Federico II", Complesso Monte S.Angelo, Via Cintia, 80126 Napoli, Italy, and Basell Polyolefins, Centro Ricerche G. Natta, P. le G. Donegani 12, I-44100 Ferrara, Italy

Received May 14, 2005; Revised Manuscript Received August 7, 2005

ABSTRACT: Highly isotactic polypropylene samples, containing a very low amount of *rr* stereodefects (0.1−0.2%) and slightly higher concentration of defects of regioregularity (0.8−0.9% of 2,1 erythro units), with different molecular masses have been prepared with an isospecific but not fully regioselective metallocene catalyst. The effects of the presence of *rr* defects and of 2,1 regiodefects and the effect of the molecular mass on the mechanical properties and crystallization behavior of polypropylene have been analyzed. Samples containing 2,1 regiodefects are very stiff and much more fragile than the samples containing only *rr* stereodefects. The presence of *rr* defects, even for low concentrations, produces instead increase of ductility and improvement of drawability at room temperature. The different effect of stereo- and regiodefects is probably related to their different levels of inclusion inside the crystalline phase. The uniform inclusion of *rr* defects in the crystals makes the stereodefective and regioregular samples more homogeneous, where crystalline and amorphous phases have the same composition. The study of the crystallization behavior has shown that the molecular mass strongly influences the amount of α and γ forms that crystallize from the melt. Samples containing regiodefects and with high molecular masses (higher than 200 000) show the same amount of γ form and the same crystallization rate. A lower amount of γ form and higher crystallization rates are instead observed for the sample having similar microstructure but lower molecular mass. This indicates that the crystallization of the γ form is favored over the α form when the crystallization is slow, that is, for samples with high molecular mass. When the molecular mass is lower than 100 000, the crystallization is faster and the formation of the α form is kinetically favored. The comparison with regioregular samples containing only *rr* stereodefects has shown that the effects of *rr* stereodefects and 2,1 regiodefects on the crystallization properties of polypropylene are very similar, at least when the concentration of defects is small (1% of *rr* stereodefects or 2,1 erythro units). Both defects produce a shortening of the regular crystallizable isotactic and regioregular sequences, inducing crystallization of the γ form.

Introduction

The crystal structure, the polymorphic behavior, and the physical properties of polypropylene strongly depend on the microstructure of the chains.[1−6] Single-center metallocene catalysts allow a perfect control over the microstructure of polypropylene chains,[7] and isotactic polypropylene (i-PP) samples characterized by different kinds and amounts of regio- and stereoirregularities, different distributions of defects, and different molecular weights can be produced.[7] As a consequence, polypropylenes with different melting temperatures having physical properties of stiff thermoplastic materials or of thermoplastic elastomers can be obtained.[5]

The relationships between microstructure, crystal structure, and physical properties of i-PP are rather complex and difficult to clarify since, depending on the used catalysts and the corresponding polymerization mechanism, different types of microstructural defect (regio- and stereoirregularities) may be, generally, contemporarily present and may produce, in principle, a different influence on the thermodynamic stability and kinetic of crystallization of the different polymorphic forms of i-PP and on the physical properties. Isolated defects of stereoregularity generating a *rr* triad, and defects of regioregularity due to secondary 2,1 insertions of monomer in a prevailing primary 1,2 enchainment, are shown as an example in Scheme 1.

Scheme 1. Isolated *rr* Triad Stereodefect in an Isotactic Chain Segment (A), 2,1-Erythro (B), and 2,1-Threo (C) Regioerrors

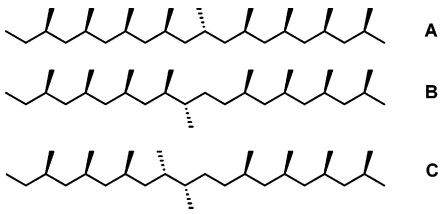

Clarifying the effect of the presence of a single type of microstructural defect on the structure and physical properties of i-PP is of great interest because it may allow increasing our control over the microstructure and the properties of polypropylene. Recent results of the researches on single-center metallocene catalysts encourage pursuing this objective. In fact, highly isospecific but not fully regioselective catalysts or less isospecific but fully regioselective catalysts are now available. For instance, Spaleck's catalysts[8] of general

† Università di Napoli "Federico II".
‡ Basell Polyolefins.
* To whom correspondence should be addressed: Tel ++39 081 674346; Fax ++39 081 674090; e-mail claudio.derosa@unina.it, derosa@chemistry.unina.it.

10.1021/ma051004x CCC: $30.25
Published on Web 10/08/2005

Chart 1. Structures of the C_2-Symmetric (1, 2) and C_1-Symmetric (3) *ansa*-Zirconocene Catalysts

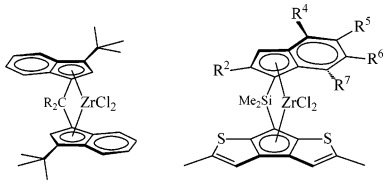

1: R = H, **2**: R = CH_3

3: R^2 = Me, Et, Ph
R^4 = Me, Ph
R^5 = H, or R^4R^5 = benzo
R^7 = H, Me

structure *rac*-Me_2Si(2-methyl-4-arylindenyl)$_2ZrCl_2$ produces polypropylenes of very high isotacticities (*mmmm* ≥ 99%),[7] with a very small amount of stereodefects, but containing 0.5−1% of regiodefects (isolated 2,1 erythro units). Fully regioselective catalysts of variable isoselectivity have been described by Resconi et al.[9−15] (Chart 1). For instance, the C_2-symmetric complexes **1** and **2** of Chart 1, of structure *rac*-R_2C(3-*t*-butylindenyl)$_2ZrCl_2$,[9,10] produce i-PP of relatively high isotacticities (*mmmm* = 95−97%), while the C_1-symmetric *ansa*-zirconocenes (**3** of Chart 1), characterized by the (substituted indenyl)-dimethylsilyl[bis(2-methylthieno)-cyclopentadienyl] ligand framework,[11−15] produce fully regioregular polypropylenes with largely variable degree of isotacticity, depending on the pattern of indene substitution.

Chains of i-PP samples prepared with both C_2- and C_1-symmetric catalysts of Chart 1 are characterized by a very simple microstructure since they contain only one type of defect, that is, stereoirregularities due to the presence of isolated *rr* triads.[9−15] The designed catalysts have allowed us studying the effect of the presence of *rr* defects on the polymorphic behavior and mechanical properties of i-PP.[5] These samples have provided the first example of metallocene-made i-PP with a random distribution of defects, not including regioerrors and with a content of stereoerrors spanning a wide range.[5,9−15]

These studies have generated a unified view of the crystallization of metallocene-made i-PP.[1,2,4−6] i-PP crystallizes from the melt as a mixture of crystals of α and γ forms, and the content of γ form increases with increasing concentration of defects due to the reduced length of the regular isotactic sequences.[1,2,5] The presence of *rr* defects induces crystallization of γ form and of disordered modifications intermediate between α and γ forms. A linear relationship between the amount of γ form that crystallizes from the melt and the average length of isotactic sequences has been found.[5] Depending on the concentration of *rr* defects, polypropylenes with melting temperatures variable from 160 to 80 °C and mechanical properties intermediate between those of stiff-plastic and elastomeric materials have been produced.[5]

Different types of microstructural defects (stereo- and regiodefects) may give in principle a different influence on the crystallization behavior and mechanical properties of i-PP. After the study of the effect of *rr* stereodefects on the physical properties of i-PP reported in our previous paper,[5] we have studied the effect of the presence of regiodefects with the aim to discriminate the influence of stereo- and regiodefects on the polymorphic behavior and mechanical properties of i-PP. The fine-tuning of the microstructure is indeed possible through the rational choice of the catalytic system,[7] and i-PP samples containing only *rr* defects or only regiodefects can be easily prepared by using a suitable metallocene catalyst. The study of the influence of regiodefects on the physical properties of i-PP is shown in this paper.

Highly stereoregular samples of i-PP have been prepared with highly isospecific but not fully regiospecific catalysts. These samples have different molecular masses and are characterized by the presence of defects of regioregularity due to secondary insertions of the monomer in a prevailing primary propylene enchainment (isolated 2,1 erythro units). The effects of the presence of defects of regioregularity and of the molecular weight on the polymorphic behavior and the mechanical properties of i-PP are compared with the effect of the presence of *rr* stereodefects described in our recent paper.[5]

Experimental Section

The analyzed samples of i-PP are listed in Table 1. The samples iPP1−iPP5 have been prepared in the laboratories of Basell Polyolefins with a highly stereospecific, not fully regiospecific catalyst, activated with methylalumoxane (MAO). The MAO-activated complexes were supported on porous polyethylene spheres as described in the literature.[16] These samples present similar melting temperatures (nearly 150 °C) and isotacticities (*mmmm* ≈ 99%), with a very small amount of *rr* defects (0.1−0.2%) and a slightly higher amount of regiodefects due to secondary insertions of propylene (0.8−0.9% of 2,1-erythro units), but different molecular masses, variable in the range 68 000−600 000 (Table 1). The different molecular masses have been obtained operating with a different H_2 pressure.

The crystallization behavior and the mechanical properties of these regioirregular samples iPP1−iPP5 are compared with the data obtained for highly regioregular and stereodefective samples prepared with the C_2- and C_1-symmetric zirconocene catalysts **1**, **2**, and **3** of Chart 1.[5] In particular, the mechanical properties are compared with a highly isotactic sample (iPP6), prepared with the catalyst **1**, *rac*-H_2C(3-*t*-butylindenyl)$_2ZrCl_2$,[10] activated with MAO (Table 1). This sample contains only 0.49% of *rr* stereodefect with no detectable regioerrors (2,1 insertions).

All propylene polymerizations have been performed in liquid propylene at polymerization temperatures between 50 and 70 °C, as described in refs 9−15.

The microstructural data of all i-PP samples have been obtained from ^{13}C NMR analysis. ^{13}C NMR spectra were acquired on a DPX-400 spectrometer operating at 100.61 MHz in the Fourier transform mode at 120 °C. The peak of the *mmmm* pentad carbon was used as internal reference at 21.8 ppm. The samples were dissolved in 1,1,2,2-tetrachloroethane-d_2 at 120 °C with a 8% w/v concentration in a 5 mm tube. Each spectrum was acquired with a 90° pulse, 12 s of delay between pulses, and CPD (WALTZ 16) to remove $^1H-^{13}C$ coupling. About 2500 transients were stored in 32K data points using a spectral window of 6000 Hz. Statistical modeling of pentad distributions of the samples was satisfactorily done using a model based on enantiomorphic site control.

The intrinsic viscosity [η] was measured in tetrahydronaphthalene at 135 °C using a standard Ubbelohde viscosimeter. The average molecular weights of the i-PP samples were obtained from their intrinsic viscosity values according to $[\eta] = K(\bar{M}_v)^\alpha$, with $K = 1.93 \times 10^{-4}$ and $\alpha = 0.74$.[17]

The SEC curves of the i-PP samples show narrow molecular weight distributions, with $M_w/M_n = 2-3$, typical of single-center zirconocene catalysts (Figure 1). The sample iPP4 presents a bimodal distribution of the molecular masses with two maxima in the SEC curve centered at low and high values of the molecular mass (30 000 and 700 000) with polydispersity $\bar{M}_w/\bar{M}_n = 15.5$ (Figure 1). This sample has been prepared in the same polymerization conditions but introducing hydrogen

Table 1. Polymerization Temperatures (T_p), Viscosity-Average Molecular Masses ($\bar{M}_v$), Weight-Average Molecular Masses ($\bar{M}_w$), Polydispersities ($\bar{M}_w/\bar{M}_n$), Melting Temperatures (T_m), Content of Experimental Triads Stereosequences (%), Enantiomorphic Model Triad Test (E), and Concentration of Secondary 2,1-Erythro Units (2,1E) of the Analyzed i-PP Samples[a]

sample	T_p (°C)	$\bar{M}_v$[b]	$\bar{M}_w$[c]	$\bar{M}_w/\bar{M}_n$[c]	T_m (°C)[d]	[*mm*] (%)	[*mr*] (%)	[*rr*] (%)	E[e]	2,1E (%)
iPP1	70	577 300	629 000	2.9	150	99.57	0.28	0.14	1.00	0.88
iPP2	70	590 600	n.d.	n. d.	150	99.45	0.38	0.17	0.86	0.86
iPP3	70	205 800	237 500	2.2	150	99.31	0.45	0.24	1.09	0.82
iPP4	70	328 000	568 000	15.5	151	n.d[f]	n.d.[f]	n.d.[f]	n.d.[f]	n.d.[f]
iPP5	70	68 400	85 000	2.8	151	99.41	0.40	0.19	0.95	0.81
iPP6	50	195 700	236 800	2.8	162	98.54	0.98	0.48	0.98	0

[a] Samples iPP1−iPP5 have been prepared with the same highly isospecific but not fully regiospecific catalyst, whereas the sample iPP6 has been prepared with the regiospecific catalyst **1**/MAO of Chart 1. [b] Viscosity-average molecular masses were obtained from the intrinsic viscosity values according to $[\eta] = K(\bar{M}_v)^\alpha$, with $K = 1.93 \times 10^{-4}$ and $\alpha = 0.74$.[17] [c] Weight-average molecular masses and polydispersities were obtained from the SEC curves. [d] Melting temperatures from DSC scans at heating rate of 10 °C/min. [e] $E = 2[rr]/[mr]$. [f] n.d = not determined.

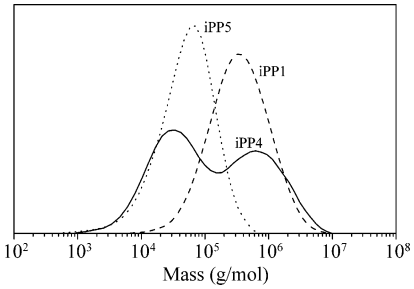

Figure 1. Comparison between the GPC curves of samples iPP1 (dashed line), iPP5 (dotted line), and iPP4 (continuous line), showing monomodal and bimodal molecular mass distributions.

only after 30 min from the beginning of the reaction, and polymerizing in the presence of H_2 for an additional 10 min, so that chains with high molecular mass are obtained in the first step of the polymerization, without H_2, whereas chains with lower molecular mass are obtained in the presence of hydrogen.

The calorimetric measurements were performed with a differential scanning calorimeter (DSC), Mettler DSC-20, in a flowing N_2 atmosphere. The melting temperatures of the samples were taken as the peak temperature of the DSC curves recorder at 10 °C/min.

The various i-PP samples were isothermally crystallized from the melt at different temperatures. Compression-molded specimens were melted at 200 °C and kept for 5 min at this temperature in a N_2 atmosphere; they were then rapidly cooled to the crystallization temperature, T_c, and kept at this temperature, still in a N_2 atmosphere, for a time long enough to allow complete crystallization at T_c. The samples were then rapidly cooled to room temperature and analyzed by X-ray diffraction.

The kinetics of crystallization from the melt of the i-PP samples were studied performing melt-crystallizations at different temperatures in a differential scanning calorimeter Mettler DSC-20. Powder samples were melted at 200 °C and kept for 5 min at this temperature in a N_2 atmosphere; they were then rapidly cooled to the crystallization temperature, T_c, and kept at this temperature, still in a N_2 atmosphere, for a crystallization time t. The samples were then heated from T_c up to 200 °C at heating rate of 10 °C/min, while recording the melting enthalpy of the material crystallized at the temperature T_c during the time t, $\Delta H(t)$. The degree of crystallinity was calculated as a function of the crystallization time as $x_c(t) = \Delta H(t)/\Delta H_m°$ with the thermodynamic melting enthalpy of i-PP in the α form, $\Delta H_m° = 209.5$ J/g.[18] It is worth noting that Mezghani and Phillips[19a] and Bond and Spruiell[20] obtained a slightly lower value of $\Delta H_m{}^0 = 167$ J/g for the equilibrium melting enthalpy of α form of i-PP. In the present context a different choice for the $\Delta H_m{}^0$ value would not affect our results, since the $\Delta H_m°$ value of the α form is used for a rough evaluation of the degree of crystallinity. In fact, we are interested in establishing the values of semicrystallization time ($t_{1/2}$) of the whole crystallizable material (time at which half of the crystallizable materials is crystallized in isothermal conditions), regardless of the number and the amount of crystalline forms, which develop at any crystallization temperature. In fact, the kinetics and the values of $t_{1/2}$ are not affected by a more quantitative analysis, for instance taking into account the crystallization of the small amount of γ form.

X-ray powder diffraction profiles were obtained with Ni-filtered Cu Kα radiation with an automatic Philips diffractometer. The relative amount of crystals in the γ form present in our samples was determined from the X-ray diffraction profiles, by measuring the ratio between the intensities of the $(117)_\gamma$ reflection at $2\theta = 20.1°$, typical of the γ form, and the $(130)_\alpha$ reflection at $2\theta = 18.6°$, typical of the α form: $f_\gamma = I(117)_\gamma/[I(130)_\alpha + I(117)_\gamma]$. The intensities of $(117)_\gamma$ and $(130)_\alpha$ reflections were measured from the area of the corresponding diffraction peaks above the diffuse amorphous halo in the X-ray powder diffraction profiles. The amorphous halo has been obtained from the X-ray diffraction profile of an atactic polypropylene, and then it was scaled and subtracted from the X-ray diffraction profiles of the melt-crystallized samples. The X-ray degree of crystallinity has been evaluated from the X-ray powder diffraction profiles by the ratio of the crystalline diffraction area and the total area of the diffraction profile.

Mechanical tests have been performed at room temperature on compression-molded films with a miniature mechanical tester apparatus (Minimat, by Rheometrics Scientific), following the standard test method for tensile properties of thin plastic sheeting ASTM D882-83. Compression-molded films have been prepared by heating powder samples at temperatures higher than the melting temperatures between perfectly flat brass plates under a press at very low pressure and slowly cooling (at nearly 10 °C/min) to room temperature. Special care has been taken to obtain films with uniform thickness (0.3 mm) and minimize surface roughness, according to the recommendation of the standard ASTM D-2292-85.

Rectangular specimens 10 mm long, 5 mm wide, and 0.3 mm thick have been stretched up to the break. The ratio between the drawing rate and the initial length was fixed equal to 0.1 mm/(mm min) for the measurement of Young's modulus and 10 mm/(mm min) for the measurement of stress−strain curves and the determination of the other mechanical properties (stress and strain at break). The reported values of the mechanical properties are averaged over at least five independent experiments.

Results and Discussion

Structural Analysis and Crystallization Kinetics. The nature and distribution of chain defects in the i-PP samples of Table 1 have been determined by ^{13}C NMR. The methyl region of the ^{13}C NMR spectrum of the sample iPP2 is presented in Figure 2 as an example. The presence of resonances of methyl carbon atoms related to the 2,1-erythro regiodefects (2,1E) is apparent (6 and 8 at ≈17.1 and 17.5 ppm, respectively). The

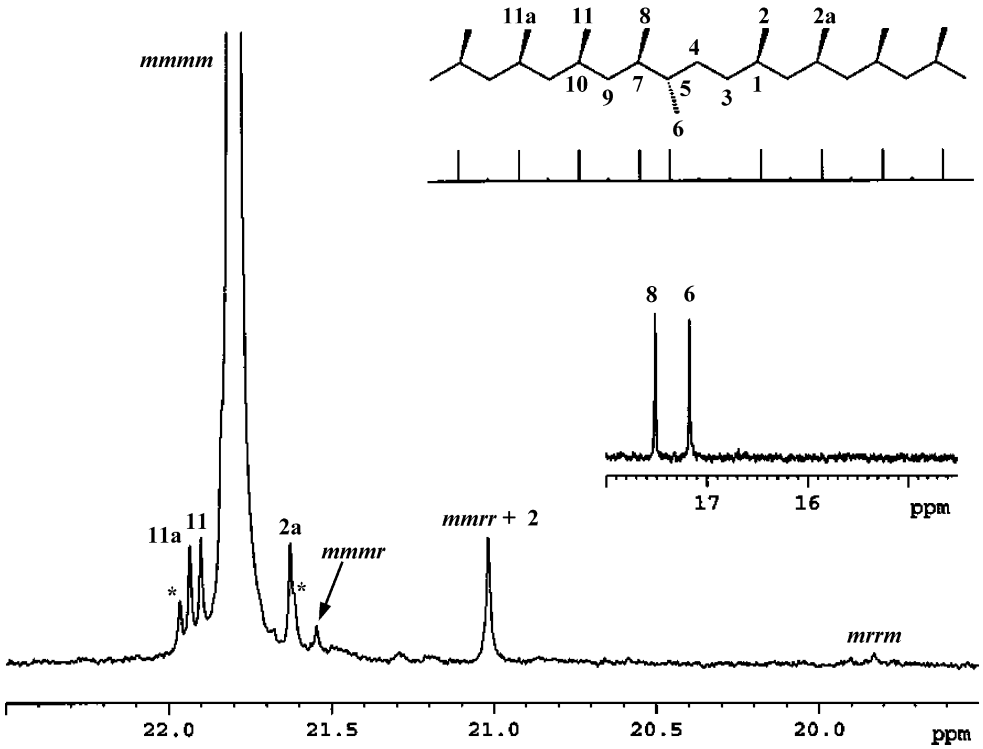

Figure 2. Methyl region of the ^{13}C NMR spectrum of the sample iPP2, showing the peaks related to 2,1 erythro regiodefects and signals corresponding to pentad stereosequences. Peaks marked with an asterisk are the $^{13}C-^{13}C$ satellites of the most intense *mmmm* resonance.

Table 2. Experimental Concentration of Pentads Stereosequences (%) of the Regiodefective i-PP Samples

sample	*mmmx* (%)	*rmmr* (%)	*mmrr* (%)	*xmrx* (%)	*rmrm* (%)	*rrrr* (%)	*rrrm* (%)	*mrrm* (%)
iPP1	99.57	0.00	0.28	0.00	0.00	0.00	0.00	0.14
iPP2	99.45	0.00	0.38	0.00	0.00	0.00	0.00	0.17
iPP3	99.31	0.00	0.45	0.00	0.00	0.00	0.00	0.24
iPP5	99.41	0.00	0.40	0.00	0.00	0.00	0.00	0.19

Table 3. Concentration of 2,1-Erythro Regioerrors (2,1E), Calculated Concentration of Pentads Stereosequences (%), Least-Squares Values for the Enantiomorphic Site Model (LS), and Total Concentration of Defects (ϵ) of the Analyzed i-PP Samples

sample	2,1E (%)	*mmmm* (%)	*mmmr* (%)	*rmmr* (%)	*mmrr* (%)	*xmrx* (%)	*rmrm* (%)	*rrrr* (%)	*rrrm* (%)	*mrrm* (%)	LS	ϵ^a (%)
iPP1	0.88	99.291	0.283	0.000	0.283	0.001	0.000	0.000	0.000	0.141	2.512×10^{-10}	1.02
iPP2	0.86	99.077	0.368	0.000	0.368	0.001	0.001	0.000	0.001	0.184	6.100×10^{-8}	1.04
iPP3	0.82	98.857	0.455	0.001	0.455	0.002	0.001	0.001	0.001	0.228	3.384×10^{-8}	1.05
iPP5	0.81	99.013	0.393	0.000	0.393	0.002	0.001	0.000	0.001	0.197	1.067×10^{-8}	1.01
iPP6	0	97.55	0.97	0.00	0.97	0.01	0.00	0.00	0.00	0.49	8.57×10^{-1}	0.49

[a] $\epsilon = [mrrm] + [2,1E]$.

experimental triad distribution and the enantiomorphic model triad test ($E = 2[rr]/[mr]$, $E = 1$ for perfect site control) are reported in Table 1.

The *mmmm* content was obtained modeling the experimental pentad distribution with the enantiomorphic site model. The experimental pentad distribution used as the starting point for the modeling is obtained from the pentad methyl region excluding the contribution of propylene units being not part of *mmmm and mmrr* pentads of head-to-tail PPPPP propylene sequences (carbons 2a, 2, and 11 in Figure 2). In particular, the *mmmm* + *mmmr* area was obtained from the integral of the region between 22 and 21.40 ppm subtracting twice the area of methylene 9 (the peak of 9 is at 42.14 ppm), and the *mmrr* pentad was obtained from the area at 21.01 ppm subtracting the contribution of 9. The so-obtained experimental pentad distribution, for the regioirregular samples iPP1−iPP5, is reported in Table 2.

The content of 2,1 errors (Table 1) was obtained as [2,1E] = 100 × (area of 9/ΣCH_2 area).

As the enantiomorphic model triad test was found close to 1 for all samples (Table 1), the experimental pentad distribution was satisfactorily fitted with the simple enantiomorphic site model. The calculated pentad distribution, the least-squares values, and the total concentration of defects, $\epsilon = [mrrm] + [2,1E]$, are collected in Table 3.

Samples iPP1−iPP5 are characterized by different molecular masses, variable in the range 68 000−600 000, and similar concentration of *rr* triad defects (0.1−0.2%) and regiodefects (0.8−0.9% of 2,1 erythro units). The sample iPP6, prepared with the catalyst **1**/MAO, is instead characterized by only *rr* defects

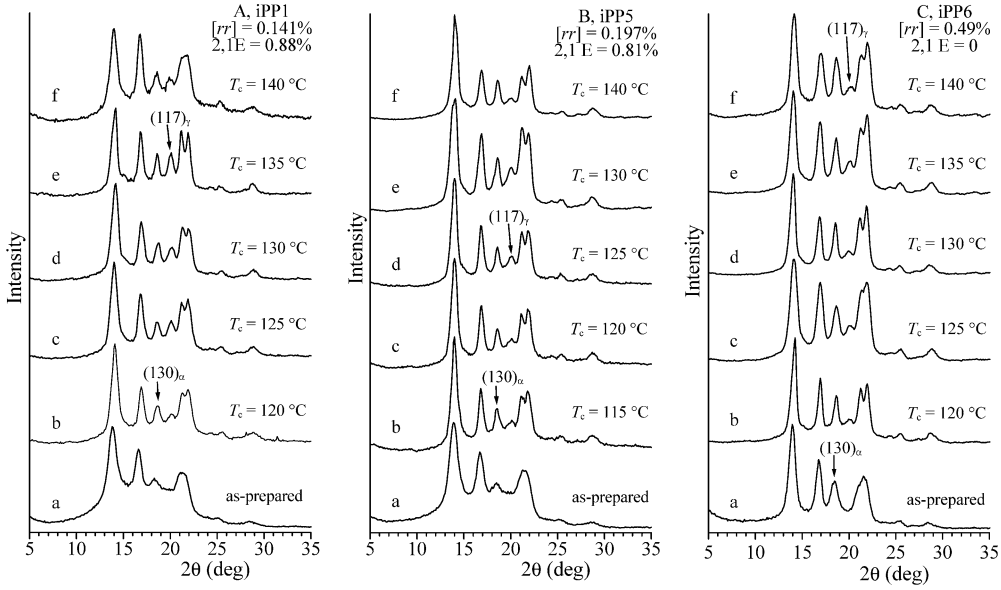

Figure 3. X-ray powder diffraction profiles of some i-PP samples of Table 1 isothermally crystallized from the melt at the indicated temperatures. The $(130)_\alpha$ reflection of the α form at $2\theta = 18.6°$ and the $(117)_\gamma$ reflections of the γ form at $2\theta = 20.1°$ are indicated.

(0.49%) and the absence of any detectable regiodefects. The amount of *rr* defects in the regioregular sample iPP6 is slightly higher than that of the regioirregular samples iPP1−iPP5 (Table 3).

The comparison of the polymorphic behavior of samples iPP1−iPP5 with that of the sample iPP6 allows comparing the effect of the presence of regiodefects and stereodefects on the crystallization properties of i-PP.

Samples of Table 1 have been isothermally crystallized from the melt at different crystallization temperatures and analyzed by X-ray diffraction. The X-ray powder diffraction profiles of melt-crystallized specimens of three samples are reported in Figure 3. The diffraction profiles of the as-prepared samples are also reported in Figure 3 (profiles *a*) for comparison.

The as-prepared sample iPP6 is crystallized basically in the α form, as indicated by the presence and the high intensity and sharpness of the $(130)_\alpha$ reflection at $2\theta = 18.6°$ of the α form,[21] and the absence of the $(117)_\gamma$ reflection of the γ form at $2\theta = 20.1°$, in the X-ray powder diffraction profile *a* of Figure 3C. As-prepared specimens of the samples iPP1−iPP5 containing regiodefects are instead crystallized in α/γ disordered modifications intermediate between α and γ forms, characterized by the packing of bilayers of chains with axes either parallel, as in the α form, or perpendicular, as in the γ form.[1,2,4] This is indicated by the very low intensity of the $(130)_\alpha$ reflection at $2\theta = 18.6°$ of the α form in the X-ray diffraction profiles *a* of Figure 3A,B.[4]

All samples crystallize from the melt in mixtures of α and γ forms because the diffraction profiles of Figure 3 show the presence of both $(130)_\alpha$ and $(117)_\gamma$ reflections at $2\theta = 18.6°$ and 20.1° of α and γ forms, respectively. For each sample, the fraction of γ form with respect to the α form generally increases with increasing the crystallization temperature, as indicated by the increase of the $(117)_\gamma$ reflection of the γ form with increasing the crystallization temperature in the diffraction profiles of Figure 3.

The relative amount of the γ form with respect to the α form, f_γ, in the various samples, evaluated from the intensities of $(117)_\gamma$ and $(130)_\alpha$ reflections, is reported in Figure 4 as a function of the crystallization temperature. As already observed in the literature,[1−3,5,22−27]

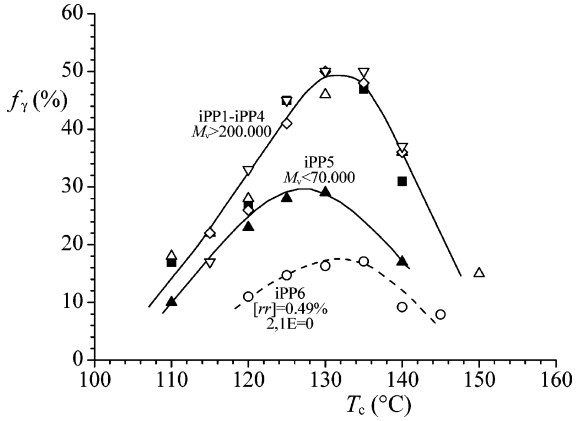

Figure 4. Relative content of γ form of i-PP, f_γ, evaluated from the X-ray diffraction profiles, in the samples of Table 1 isothermally crystallized from the melt, as a function of the crystallization temperature T_c: (■) sample iPP1, [*rr*] = 0.141%, 2,1E = 0.88%; (▽) sample iPP2, [*rr*] = 0.184%, 2,1E = 0.86%; (△) sample iPP3, [*rr*] = 0.228%, 2,1E = 0.82%; (◇) sample iPP4; (▲) sample iPP5, [*rr*] = 0.197%, 2,1E = 0.81%; (○) sample iPP6, [*rr*] = 0.49%, 2,1E = 0. Samples iPP1−iPP4 have molecular masses higher than 200 000, whereas the sample iPP5 has molecular mass lower than 70 000. Samples containing stereo- and regiodefects (iPP1−iPP5, continuous lines) are compared to sample iPP6 containing only *rr* stereodefects (dashed line).

for each sample the content of γ form increases with increasing crystallization temperature. For these samples containing relatively low total concentration of defects (1%), a maximum amount of γ form is obtained at crystallization temperatures of 130−135 °C.

In the case of samples iPP1−iPP5 containing regiodefects, the data of Figure 4 clearly indicate that the four samples having high molecular masses (higher than 200 000, samples iPP1−iPP4, Table 1) show the same polymorphic behavior. Similar amounts of γ form are, indeed, obtained in the melt-crystallizations, and a maximum amount of nearly 50% is achieved. A lower amount of γ form is instead obtained for the sample iPP5, having lower molecular mass, the maximum concentration of γ form being only 25−30%. Since the five samples present the same concentration of defects of regio- and stereoregularity, the different polymorphic

behavior of the sample iPP5 should be related to the different molecular mass. When the molecular mass is higher than 200 000, the amount of crystallized γ form is independent of the molecular mass (at least in the range 200 000−600 000), whereas with decreasing the molecular mass below 100 000 the amount of γ form decreases and the crystallization of the α form is favored.

It is worth noting that the sample iPP4 with a bimodal distribution of molecular masses (Figure 1) presents the same concentration of γ form as the high molecular mass samples iPP1−iPP3 (Figure 4). This indicates that the polymorphic behavior is mainly regulated by the chains having higher molecular mass.

It is also apparent from Figure 4 that the samples containing defects of regioregularity of high molecular masses (samples iPP1−iPP4) present amounts of γ form higher than that of the sample iPP6 containing only defects of stereoregularity, at any crystallization temperature. The sample iPP6 has a slightly higher amount of *rr* defects (0.49%) and molecular mass similar to that of the sample iPP3 and crystallizes basically in the α form with a maximum amount of γ form of only 10−15%. The higher amount of γ form obtained for the regioirregular samples iPP1−iPP4 should be related to the presence of regiodefects (2,1 erythro units). These samples, indeed, contain a total concentration of defects ϵ of nearly 1% (0.1−0.2% of *rr* stereodefects plus 0.8−0.9% of 2,1E regiodefects, see Table 3), which is twice the total concentration of defects of the sample iPP6 (only 0.49% of *rr* defects). The higher concentration of defects in samples iPP1−iPP4, even though the content of *rr* defects is lower, produces a higher amount of γ form. This indicates that, as already observed in the literature,[23,24] the presence of 2,1E regiodefects also induces crystallization of the γ form.

The data of Figure 4 show that both *rr* stereodefects and 2,1E regiodefects influence the crystallization behavior of i-PP, inducing crystallization of the γ form. In recent papers it has been demonstrated that the relative stability of α and γ forms of i-PP is related to the concentration of defects and, hence, to the average length of the fully isotactic sequences comprised between two successive interruptions.[1−3,5,22−24] The γ form is favored when the regular isotactic sequences are short. The shorter the average length of isotactic sequences, the higher the maximum amount of γ form that can be obtained in the melt-crystallization. The length of regular isotactic sequences, in turn, depends on the amount and distribution of defects.[1,2,5,24,28] For metallocene-made i-PP samples the distribution of defects along the polymer chains is random; hence, the average length of the fully isotactic sequences, $\langle L_{iso}\rangle$, is inversely proportional to the total content of microstructural defects. Moreover, the structural analysis of i-PP samples containing only *rr* defects in a wide range of concentration has allowed finding a linear relationship between the maximum amount of γ form and the average length of the fully isotactic sequences,[5] which can be easily evaluated for these samples from the ^{13}C NMR data as $\langle L_{iso}\rangle = (2[mm]/[mr]) + 2$, at least in the range of $\langle L_{iso}\rangle = 15-170$ monomeric units. This relationship is redrawn from ref 5 in Figure 5.

In the case of the regioirregular samples of Table 1 containing *rr* stereodefects and 2,1E regiodefects the average length of regular isotactic sequences can be roughly evaluated as $\langle L_{iso}\rangle = 1/\epsilon$, where $\epsilon = [mrrm] +$ 2,1E is the total concentration of defects (Table 3). The maximum amount of γ form, f_γ(max), obtained for the regioirregular samples of high molecular mass of Table 1 from the data of Figure 4 is reported in Figure 5 as a function of the average length of the fully isotactic sequences $\langle L_{iso}\rangle$. It is apparent that the data of f_γ(max) obtained for the samples containing regiodefects are well-interpolated on the linear relationship obtained in ref 5 with the i-PP samples containing only *rr* stereodefects. This indicates that *rr* stereodefects and 2,1E regiodefects give the same influence on the crystallization of the γ form, at least for low concentrations of stereo- and regiodefects. In fact, it is reasonable to assume that for low concentration of defects (lower than 1%) *rr* stereodefects and 2,1E regiodefects give a similar effect of reducing the length of regular isotactic sequences.[2,5,24] In particular, the data of ref 5 and of Figure 5 indicate that samples of i-PP containing only *rr* defects in concentrations similar to the total amount of defects ϵ of the samples iPP1−iPP4 (nearly 1%) develop the same amount of γ form (nearly 50%) as the regiodefective samples iPP1−iPP4. For higher concentration of *rr* defects, instead, the influence of *rr* defects on the crystallization behavior is not only limited to shorten the regular isotactic sequences but is also related to the inclusion of this stereodefect in the crystals of the polymorphic forms of i-PP,[4,6,25,30] in particular the easy inclusion in the crystal lattice of γ form.[4,6]

The data of Figures 3 and 4 show that for the sample iPP5, having the same concentration of *rr* stereodefects and 2,1E regiodefects as samples iPP1−iPP4 but lower molecular mass, a lower amount of γ form is obtained. Recent literature data[24] have shown that the content of γ form, which develops by isothermal crystallization of i-PP samples having similar content of stereo- and regiodefects (i.e., 0.97% stereodefects and 0.60% regiodefects due to 2,1 erythro addition) but different molecular mass (in the range 41 000−290 000) is similar and independent of the molecular mass. Our results, instead, indicate that also the molecular mass play a role in the crystallization behavior of i-PP, at least when the concentration of defects is lower than 1%.

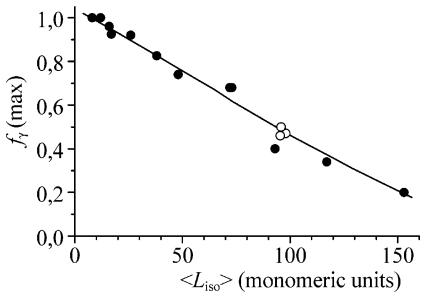

Figure 5. Relationship between the maximum amount of γ form, f_γ(max), crystallized upon melt-crystallization procedures, and the average length of fully isotactic sequences $\langle L_{iso}\rangle$ obtained in ref 5 for samples of i-PP prepared with the catalysts **1**−**3** of Chart 1 and characterized by the presence of variable amount of *rr* stereodefects (●). For these samples the values of $\langle L_{iso}\rangle$ are inversely proportional to the content of *rr* errors and has been evaluated from the ^{13}C NMR data,[5] as $\langle L_{iso}\rangle = (2[mm]/[mr]) + 2$. With the open symbol (○) are shown the data of the maximum amount of γ form, f_γ(max), obtained for the regioirregular samples iPP1−iPP4 of high molecular mass of this paper. In this case $\langle L_{iso}\rangle = 1/\epsilon$, where ϵ is the total concentration of defects $\epsilon = [mrrm] +$ 2,1E (Table 3). The data of the sample iPP5 having low molecular mass and low amount of γ form are not reported.

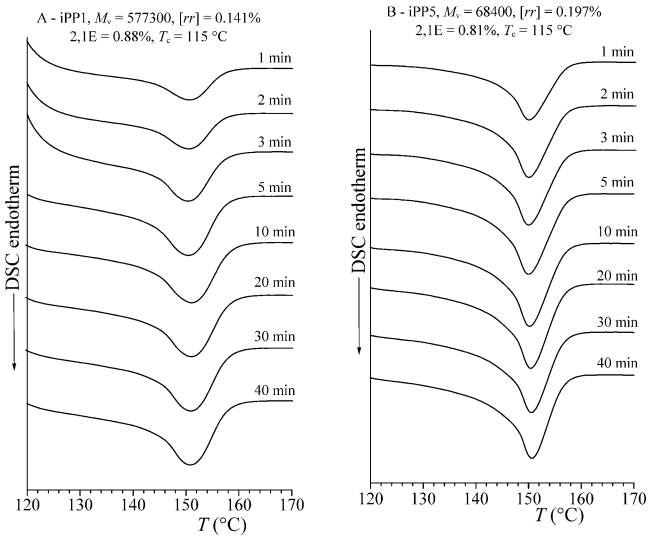

Figure 6. DSC heating scans of i-PP samples of different molecular mass isothermally crystallized from the melt at the crystallization temperature T_c = 115 °C during the indicated crystallization time: (A) sample iPP1, [*rr*] = 0.141%, 2,1E = 0.88%, M_v = 577 300; (B) sample iPP5, [*rr*] = 0.197%, 2,1E = 0.81%, M_v = 68 400.

The effect of the molecular mass is rather subtle. Lower molecular masses should, indeed, induce crystallization of the γ form because the chain ends act as defects that shorten the length of the fully isotactic sequences. This is for instance one of the special conditions that induces crystallization of a not negligible amount of γ form in the case of i-PP samples prepared with Ziegler−Natta catalysts.[28,29] The data of Figure 4, however, indicate that, for our metallocene-made i-PP, samples with low values of the molecular mass, in the range 60 000−200 000 (sample iPP5), produce by crystallization from the melt amounts of γ form lower than that obtained for samples with analogous concentration of stereo- and regiodefects but having molecular masses higher than 200 000 samples (iPP1−iPP4). This clearly indicates that the effect of shortening the length of regular isotactic sequences due to chain ends is negligible for the range of molecular masses of our samples.

The effect of molecular mass observed in Figure 4 can be, instead, explained considering that the crystallization of α and γ form of i-PP is a result of two competing kinetic and thermodynamic effects.[2,23,24] In fact, it has been demonstrated that, even in the case of samples containing an appreciable amount of stereodefects, which crystallize from the melt totally in the γ form, crystals of α form can be obtained when the crystallization is very fast, for instance by quenching the melt to room temperature.[2] The formation of the α form is therefore kinetically favored in conditions of fast crystallization.

Since the crystallization rate influences the formation of α and γ forms, the study of the effect of the molecular mass on the crystallization kinetics is of great interest. The analysis of the crystallization kinetics of samples of Table 1, having similar concentration of defects and different molecular weight, may allow clarifying the effect of the molecular weight on the crystallization rate.

Examples of crystallization kinetics for some samples of Table 1 are reported in Figures 6 and 7. The samples have been isothermally crystallized in DSC at the crystallization temperature T_c for a time t and then heated from T_c up to 200 °C at heating rate of 10 °C/min, while recording the melting enthalpy. The amount of materials crystallized at T_c during the time t has been evaluated from the measure of the melting enthalpy. The DSC heating scans from T_c after the crystallization time t are shown in Figure 6 for the samples iPP1 and iPP5 of different molecular masses and T_c = 115 °C. The difference in the crystallization kinetics is apparent. The degree of crystallinity, evaluated from the melting enthalpies in the DSC scans of the kind of Figure 6, is reported in Figure 7 as a function of the crystallization time for various crystallization temperatures. High degrees of crystallinity (40−50%) have been achieved for all samples.

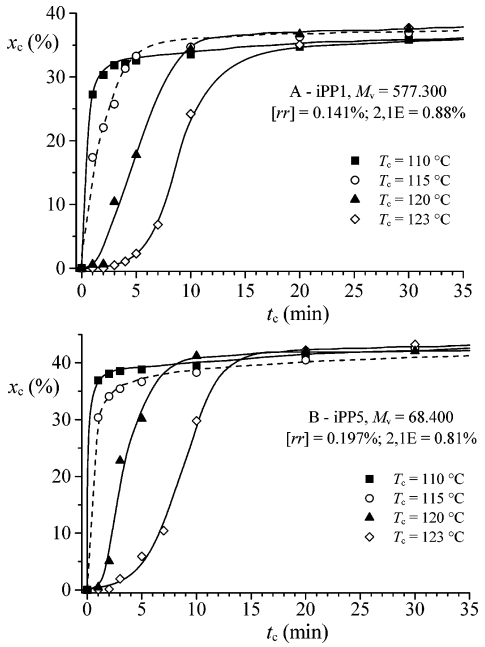

Figure 7. Degrees of crystallinity as a function of the crystallization time for i-PP samples isothermally crystallized from the melt at different crystallization temperatures T_c: (A) sample iPP1, [*rr*] = 0.141%, 2,1E = 0.88%, M_v = 577 300; (B) sample iPP5, [*rr*] = 0.197%, 2,1E = 0.81%, M_v = 68 400.

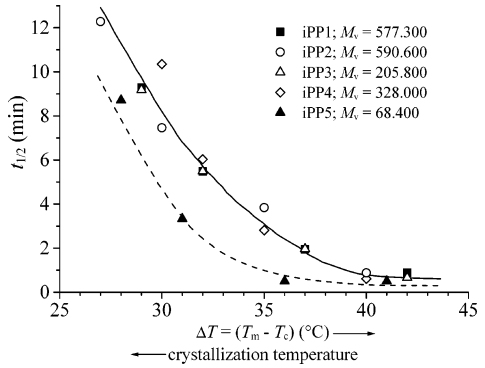

Figure 8. Semicrystallization time $t_{1/2}$ as a function of the difference between the melting temperature of the as-prepared samples and the crystallization temperature $\Delta T = (T_m - T_c)$ for i-PP samples isothermally crystallized from the melt: (■) sample iPP1, [*rr*] = 0.141%, 2,1E = 0.88%, M_v = 577 300; (○) sample iPP2, [*rr*] = 0.184%, 2,1E = 0.86%, M_v = 590 600; (△) sample iPP3, [*rr*] = 0.228%, 2,1E = 0.82%, M_v = 205 800; (◇) sample iPP4, M_v = 328 000; (▲) sample iPP5, [*rr*] = 0.197%, 2,1E = 0.81%, M_v = 68 400.

The values of the semicrystallization time $t_{1/2}$ (time at which half of the crystallizable materials is crystallized) are reported in Figure 8 as a function of the difference between the melting temperature of the as-

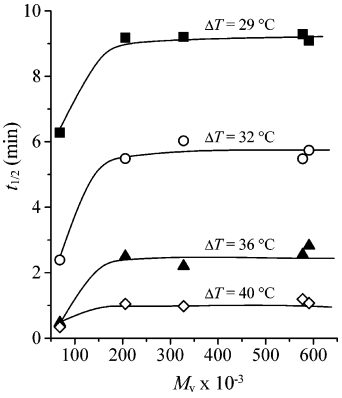

Figure 9. Semicrystallization time $t_{1/2}$ as a function the molecular mass for i-PP samples isothermally crystallized from the melt at the indicated values of $\Delta T = (T_m - T_c)$: (■) ΔT = 29 °C; (○) ΔT = 32 °C; (▲) ΔT = 36 °C; (◇) ΔT = 40 °C.

prepared samples and the crystallization temperature, $\Delta T = T_m - T_c$. Since the samples show nearly the same melting temperature, the kinetics of the different samples can be compared at the same crystallization temperature.

It is apparent that the crystallization rate is nearly the same, at any value of the crystallization temperature, for the four samples iPP1−iPP4 having higher values of the molecular weight. Moreover, at high values of ΔT (low crystallization temperatures), in condition of fast crystallization, similar crystallization rates are observed regardless of the molecular mass. At lower values of ΔT (high crystallization temperatures), instead, lower values of the semicrystallization time are observed for the sample iPP5 having the lowest molecular weight (M_v = 68 400).

The values of the semicrystallization time are reported in Figure 9 as a function of the molecular mass for various values of ΔT. The data of Figures 6−9 indicate that, for samples of i-PP having the same types and concentration of microstructural defects, the crystallization rate decreases with increasing the molecular mass in the range 60 000−200 000. For higher values of the molecular mass, in the range 200 000−600 000, the crystallization rate becomes independent of the molecular mass. The sample characterized by a bimodal distribution of the molecular mass (sample iPP4, with M_v = 328 000) shows a crystallization behavior similar to that of the samples with the highest molecular mass. The crystallization rate is mainly regulated by chains having higher molecular mass.

As expected, the effect of the molecular weight is remarkable at high crystallization temperatures (low values of ΔT), when the crystallization is slow, but it is negligible at low crystallization temperatures in condition of fast crystallization.

The kinetic data of Figures 6−9 allow explaining the structural data of Figures 3 and 4, which have shown a different polymorphic behavior of the sample iPP5 with low molecular mass, with respect to that of the samples iPP1−iPP4 having molecular masses higher than 200 000. Similar amounts of γ form are, indeed, obtained in the melt-crystallizations of samples iPP1−iPP4 and a maximum amount of nearly 50% is achieved. A lower amount of γ form is instead obtained for the sample iPP5, the maximum concentration of γ form being only 25−30%. Since the five samples present the same concentration of defects of regio- and stereoregularity, the lower amount of γ form of the sample iPP5 is probably due to its higher crystallization rate (Figure 8). When the molecular mass is higher than 200 000, the amount of crystallized γ form and the crystallization rate are independent of the molecular mass (at least in the range 200 000−600 000, Figures 4 and 9), whereas the crystallization rate increases and the amount of γ form decreases with decreasing the molecular mass below 100 000 (Figures 4 and 9). As already shown in the literature for samples containing only *rr* stereodefects,[2,5] these results may be explained considering that in i-PP samples from metallocene catalysts, containing a random distribution of defects, the crystallization of the γ form is generally favored because of the presence of defects, whereas the crystallization of the α form is kinetically favored. When the crystallization is slow, the γ form is favored over the α form. Therefore, the higher amount of γ form for samples with molecular masses higher than 200 000 is due to the decrease of the crystallization rate. When the crystallization is faster, as for the sample with low molecular mass, the crystallization of the α form is kinetically favored and the amount of crystallized γ form decreases. This is also confirmed by the fact that when the crystallization rates of all samples are similar, that is at low crystallization temperatures (Figure 8), the sample iPP5 with low molecular mass presents similar amount of γ form as the samples iPP1−iPP4 with high molecular mass (Figure 4).

In the case of the sample iPP4 with the bimodal distribution of molecular masses the crystallization rate and the polymorphic behavior are determined by the chains with higher molecular mass. The presence of a fraction of chains with very high molecular mass (around 700 000, see Figure 1) slows down the crystallization rate and favors crystallization of the γ form.

These results confirm that the crystallization of α and γ forms of metallocene-made i-PP samples containing a random distribution of defects is a result of two competing kinetic and thermodynamic effects.[2,5] The presence of defects and molecular masses higher than 70 000 favors the crystallization of the γ form. The effect of defects is the shortening the length of the regular isotactic crystallizable sequences, whereas the effect of high molecular mass is that of reducing the crystallization rate.

It is worth noting that the data on the crystallization of γ form in metallocene made i-PP samples, those for regiodefective samples presented in this paper and those for stereodefective samples reported in our previous papers,[1,2,5] are in agreement with and, in somehow, complete the extensive studies reported by Mezghani and Phillips on Ziegler−Natta i-PP samples crystallized at atmospheric and high pressures.[19] In particular, they have reported a phase diagram of highly stereoregular i-PP and have shown that the thermodynamic prediction of the formation of γ form as a function of temperature and pressure is in good agreement with experimental data.[19a] However, as discussed by Mezghani and Phillips, the phase diagram does not take into account the formation of γ form in regions where only the α form is present, due to the fact that the crystallization of the γ form is favored by the presence of defects of stereoregularity and of comonomers.[19a,c] These effects of the presence of different types of defects on the crystallization of γ and α forms have been instead studied by us in this paper and in our previous papers.[1−6]

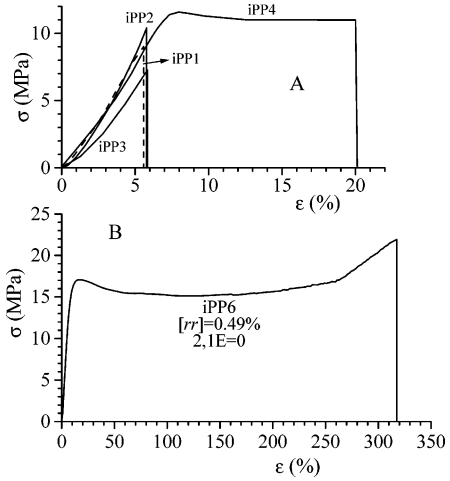

Figure 10. Stress−strain curves of compression-molded films of samples iPP1−iPP4 containing 2,1E regiodefects (A) compared to the stress−strain curve of the sample iPP6 containing only 0.49% of *rr* stereodefects (B).

Table 4. Young's Modulus (E), Stress (σ_b) and Strain (ϵ_b) at Break, Stress (σ_y) and Strain (ϵ_y) at the Yield Point, and Crystallinity of Unoriented Compression-Molded Films of Regioirregular i-PP Samples (iPP1−iPP5) Compared to the More Stereoirregular and Fully Regioregular Sample iPP6[a]

sample	M_v	*rr* (%)	2,1E (%)	E (MPa)	σ_y (MPa)	ϵ_y (%)	σ_b (MPa)	ϵ_b (%)	x_c (%)
iPP1	577 300	0.141	0.88	230			9	6	68
iPP2	590 600	0.184	0.86	233			10	6	70
iPP3	205 800	0.228	0.82	218			7	5	69
iPP4	328 000			236			11	20	70
iPP5	68 400	0.197	0.81	192			1.5	2	72
iPP6	195 700	0.49	0	198	17	16	22	310	70

[a] The contents of *rr* steredefects and 2,1E regiodefects and the molecular weights (M_v) of the samples are also indicated.

Mechanical Properties. The stress−strain curves of compression-molded films of some regioirregular i-PP samples of Table 1 are compared in Figure 10 to that of sample iPP6, containing only *rr* stereodefects. The values of the mechanical properties are reported in Table 4. The elastic modulus increases with increasing molecular mass up to a constant value for molecular masses higher than 200 000−300 000.

It is apparent from Figure 10 and Table 4 that samples iPP1−iPP5, containing 2,1E regiodefects and low amount of *rr* stereodefects, are stiff and fragile with high values of the Young's modulus and very low values of deformation at break (ϵ_b around 6%). The samples do not undergo plastic deformation at room temperature and break before yielding. This behavior is similar to that of the commercial highly isotactic polypropylene prepared with Ziegler−Natta catalysts. The sample iPP4 with a bimodal distribution of the molecular mass shows a similar behavior with a slightly higher deformation at break (ϵ_b nearly 20%), probably because the chains with lower molecular mass act as plasticizer during deformation. In fact, it is well-known from polyethylene that blending of molecular weight fractions produces better elongation at break (see for instance ref 31). Furthermore, a similar dependence of the elongation at break on the distribution of molecular weight has been observed also in the case of commercial highly isotactic polypropylene prepared with Ziegler−Natta catalysts, for fibers obtained by spinning the polymers at high spinning speeds.[32,33] In particular, the major influence of the polydispersity on the structure and properties developed by melt-spun filaments of Ziegler−Natta i-PP was attributed to its effect on both the elongational viscosity of the resin and the ability of high molecular weight tails to influence the stress-induced crystallization that occurs in the spinline.[33] According to Bond and Spruiell,[34] the narrower molecular weight distribution of metallocene i-PP resins is the primary factor that produces differences in the structure and properties of fibers spun from these resins compared to those of Ziegler−Natta i-PP samples of similar weight-average molecular mass or melt flow rate.

A completely different mechanical behavior is shown by the regioregular sample iPP6 containing only a small amount of *rr* stereodefects. In fact, while still presenting a typical behavior of stiff-plastic materials, with a high value of the elastic modulus, iPP6 shows a much higher ductility. This sample can be, indeed, stretched at room temperature up to remarkable value of the strain (ϵ_b = 320%, Figure 10), much higher than those of the regioirregular samples iPP1−iPP5. Since sample iPP6 has a molecular mass and a crystallinity similar to those of sample iPP3, the higher ductility could be attributed to the different microstructure, in particular the higher concentration of *rr* defects and the absence of 2,1 regiodefects. These data can be explained considering that *rr* defects are in part included in the crystals of α and γ forms of i-PP producing more defective crystals.[1,2,4−6,25,30] VanderHart et al.[25,30] have recently found that the concentration of *rr* defects in the crystals is reduced from their overall value by about half and that those defects which are found in the crystalline region are not strongly biased to the interface between crystal and amorphous phases; i.e., they can also be found in the interior of the crystalline regions. These defects are therefore homogeneously distributed within the crystals, and since nearly the same concentration is present also in the amorphous phase, they are homogeneously distributed inside crystalline and amorphous regions.[25,30] The samples are therefore more "morphologically" homogeneous, resulting in an improvement of drawability. Moreover, VanderHart et al.[25,30] have also found that the level of rejection of *rr* defects from the crystalline regions does not seem to depend on the crystalline form (α or γ forms). Therefore, samples containing only *rr* defects turn out to be "homogeneous" and ductile even when the concentration of *rr* defects is low, and the samples basically crystallize in the α form (as the sample iPP6, Figures 3 and 4).

We have recently shown that, in the case of i-PP samples containing only *rr* defects, a further increase of concentration of *rr* defects produces a further increase of concentration of γ form and of ductility, so that highly flexible materials are obtained for *rr* contents around 5−6 mol %, and elastomeric polypropylenes are produced for concentration of *rr* defects higher than 7 mol %.[5,6] All these materials are initially crystallized, in the unstretched compression-molded films, totally in the γ form or in disordered modifications close to the γ form.[5]

The regioirregular samples iPP1−iPP5 present a negligible amount of *rr* defects (0.1−0.2%), whereas the 2,1 regiodefects, which are probably less compatible in the crystals, are mainly segregated in the amorphous phase.[25,30] VanderHart et al.[25,30] have, indeed, recently found that the amount of 2,1 regiodefects included in the crystalline phase is much lower than that of *rr* stereodefects. Crystallization tends to reject the 2,1

regiodefects more strongly than the *rr* defects.[25] These regioirregular samples are therefore more "morphologically" heterogeneous, resulting in very stiff and more fragile materials.

The different inclusion of regio- and stereodefects inside i-PP crystals is probably related to the results of Bond and Spruiell,[20] who found that metallocene i-PP samples have lamellae thickness and heat of fusion similar to those of Ziegler−Natta i-PP samples, but present lower melting temperatures. This was attributed to the fact that metallocene-made i-PP show higher fold surface free energy (σ_e) compared to Ziegler−Natta i-PP samples due to a segregation of the chain defects in the fold surface of lamellae.[20] It was inferred that segregation of defects in the folds, higher σ_e values, and formation of γ form are somehow related.[20] Since the metallocene i-PP samples analyzed in ref 20 contained nonnegligible amounts of stereo- and regiodefects, the rejection of regiodefects outside the crystals probably plays the major role in determining higher fold surface free energy. On the other hand, it is also generally accepted that the main difference between metallocene and Ziegler−Natta i-PPs is the different distribution of defects along the polymer chains, which is more homogeneous in the case of metallocene i-PPs.[28,35] The nonuniform distribution of defects in Ziegler−Natta i-PP samples produces chains with longer defect-free regions whose crystallization results in more-ordered crystals and thicker lamellae with higher melting temperature.[28,35−38]

The different degree of incorporation of *rr* stereodefects and 2,1E regiodefects into crystals of α and γ forms of i-PP suggests that regiodefective i-PP samples (as samples iPP1−iPP5) and stereodefective and fully regioregular i-PP samples (as the sample iPP6) may be described by the limit models used by Sanchez and Eby to describe the crystalline state of random copolymers.[39,40] In fact, if the stereo- and regiodefects are considered as noncrystallizable comonomeric units (B units) and isotactic and primary 1,2 sequences of propene monomeric units as crystallizable comonomeric units (A units), stereodefective and regiodefective metallocene i-PP homopolymers can be considered as random copolymers since *rr* stereodefects and/or 2,1 regiodefects are randomly distributed along the polymer chains. Since *rr* stereodefects are easily included into crystals of α and γ form,[4,6,25,30] the crystallization of stereodefective i-PP samples may be described by the uniform comonomer inclusion model of Sanchez and Eby;[39,40] that is, the crystalline phase is a solid solution of A and B units where the B counits produce defects in the crystalline A lattice and both crystalline and amorphous phases have the same composition because the defects B (*rr* stereodefects) are uniformly distributed between crystalline and amorphous phases. In this sense, as discussed above, the stereodefective samples (as the sample iPP6) are "morphologically" homogeneous.

In the second limit model, that is the comonomer exclusion model described by Flory,[41] the crystalline phase is composed entirely of A units and is in metastable equilibrium with a mixed amorphous phase of A units and noncrystallizable B counits. Since the 2,1 regiodefects are not totally excluded from the crystals, but only partially included into crystals,[25,30] the crystalline state of regiodefective samples iPP1−iPP5 must lie between the two limit models with crystalline and amorphous phases having a nonhomogeneous composition. In this sense these samples are more "morphologically" heterogeneous.

Sanchez and Eby[39,40] have shown that, for both of these two limit models (uniform comonomer inclusion and comonomer exclusion), the crystal thickness increases linearly with increasing small concentrations of the B counits, in these cases the stereo- and regiodefects, for isothermal crystallizations carried out at the same temperature. Moreover, Sanchez and Eby[40] have also shown that this linear relationship applies not only to the extreme copolymer crystals with the comonomer units either rejected or uniformly included (as the stereodefective i-PPs) but also to crystals with intermediate concentrations (as the regiodefective i-PPs). This prediction of the Sanchez−Eby theory has been confirmed by experimental data on copolymers of L- and DL-lactides.[40,42] However, when the copolymer samples are crystallized by quenching or by cooling at uniform rate, diffusional transport effects can cause the effective undercooling at which crystallization occurs to increase with increasing comonomer (defects) concentration.[39,43] Higher undercoolings cause a decrease of crystal thickness with increasing comonomer concentration,[39] as experimentally found, for instance, in tetrafluoroethylene−hexafluoropropylene copolymers.[43−45]

The model of uniform inclusion of *rr* defects explains not only the higher ductility of the stereodefective and regioregular sample iPP6, compared to the regiodefective samples iPP1−iPP5 (Figure 10), but can also explain its higher melting temperature (162 °C, Table 1), which nearly approaches that of Ziegler−Natta i-PP samples. In fact, according to the Sanchez−Eby theory,[39,40] the kinetically controlled crystal thickness should be sufficiently high in stereodefective i-PPs even though the crystallizable regular isotactic sequences are much shorter that those of Ziegler−Natta i-PP samples, where the nonuniform distribution of defects produces chains with longer defect-free regions even in the presence of a not negligible concentration of stereodefects. Moreover, the low conformational and packing energy model of inclusion of *rr* defects in crystals of γ form that we have proposed[4] suggests that the excess enthalpy of the defect in the Sanchez−Eby theory,[39,40] created by incorporating *rr* triad defects in the crystal lattice, is probably very low, accounting for the high melting temperature of the sample iPP6 and the crystallization from the melt of a not negligible amount of γ form (Figure 4).[5] It is, instead, reasonable to assume that the excess enthalpy of the defect created by incorporating even a low amount of less compatible 2,1 regiodefects in the crystal lattice is much higher. This may explain the lower melting temperatures of regiodefective samples iPP1−iPP5 (Table 1) even though their crystal thickness is presumably not different from that of the stereodefective sample iPP6, according to the fact that the Sanchez−Eby linear relationship between defect concentration and crystal thickness applies also to systems characterized by crystalline and amorphous phases having different defects concentrations (partial comonomer inclusion).[40]

Conclusions

Highly isotactic polypropylene samples having different molecular masses have been prepared with a highly isospecific but not fully regiospecific metallocene catalyst. The samples contain a very low amount of *rr*

stereodefects (0.1−0.2%) and slightly higher concentration of defects of regioregularity due to secondary propylene insertion (0.8−0.9% of 2,1 erythro units). The similar microstructure of the produced samples has allowed studying the effect of the molecular mass on the crystallization behavior and the kinetics of melt-crystallization of polypropylene. The polymorphic behavior has been compared to that of highly regioregular i-PP sample containing only *rr* stereodefects, prepared with regiospecific C_2-symmetric metallocene catalyst. The effects of *rr* defects and of 2,1E regiodefects on the crystallization properties and mechanical properties have been compared.

All samples crystallize from the melt in mixtures of crystals of α and γ forms. Samples containing regiodefects and with high molecular masses (higher than 200 000) show the same polymorphic behavior. Similar amounts of γ form are, indeed, obtained at any crystallization temperature and a maximum amount of nearly 50% is achieved. A lower amount of γ form is instead obtained for the sample having similar microstructure but lower molecular mass, the maximum concentration of γ form being only 25−30%.

The kinetic study has shown that for these samples of i-PP having the same types and concentration of microstructural defects the crystallization rate decreases with increasing the molecular mass in the range 60 000−200 000. For higher values of the molecular mass, in the range 200 000−600 000, the crystallization rate becomes independent of the molecular mass, whereas higher crystallization rates are observed for the sample with the lowest molecular mass of 68 400.

The kinetic data explain the different polymorphic behavior observed for the sample with the lowest molecular mass. The crystallization of the γ form is favored over the α form when the crystallization is slow, that is, at high crystallization temperature or for samples with high molecular masses. Therefore, the higher amount of γ form for samples with molecular masses higher than 200 000 is due to the decrease of the crystallization rate. When the crystallization is faster, as for the sample with low molecular mass, the crystallization of the α form is kinetically favored and the amount of crystallized γ form decreases.

The comparison with i-PP samples containing only *rr* stereodefects and free from regiodefects has shown that the effects of *rr* stereodefects and 2,1E regiodefects on the crystallization behavior of i-PP are very similar, at least for low concentrations of defects (≈1%) and molecular masses higher than 200 000. The values of the maximum amount of γ form obtained for the regioirregular samples (≈50%) having a total concentration of defect of nearly 1% (stereodefects plus regiodefects) are well-interpolated by the linear relationship between the maximum amount of γ form and the average length of isotactic sequences $\langle L_{iso} \rangle$ found for samples of i-PP containing only *rr* stereodefects.[5] This indicates that when the concentration of defects is low (around 1%), *rr* defects and 2,1 regiodefects give mainly a similar effect of shortening the fully isotactic and regioregular sequences and produce development of similar concentration of γ form.

These results confirm that the crystallization of α and γ forms of metallocene-made i-PP samples containing a random distribution of defects is a result of two competing kinetic and thermodynamic effects.[2,5] The presence of defects and high molecular masses favor the crystallization of the γ form. Defects shorten the length of the regular isotactic crystallizable sequences, whereas high molecular mass reduces the crystallization rate.

The analysis of the mechanical properties has shown that the samples containing 2,1E regiodefects are very stiff and more fragile than the samples containing only *rr* stereodefects. They present, indeed, high modulus and break at very small deformations before yielding. Samples containing only *rr* defects are instead highly ductile and can be stretched at room temperature up to remarkable values of strain.[5]

These data can be explained considering that *rr* defects are uniformly included in the crystals of α and γ forms of i-PP producing more defective crystals.[1,2,4,6,25,30] As found by VanderHart et al.,[25,30] these defects are homogeneously distributed within the crystals, and since nearly the same concentration is present also in the amorphous phase, they are homogeneously distributed inside the crystalline and amorphous regions. Therefore, the stereodefective samples are more "morphologically" homogeneous, resulting in an improvement of drawability. The regioirregular samples iPP1−iPP5 present a negligible amount of *rr* defects (0.1−0.2%), whereas the 2,1 regiodefects, which are probably less compatible in the crystals, are mainly segregated in the amorphous phase.[25,30] These regioirregular samples are therefore more "morphologically" heterogeneous with crystalline and amorphous phases having different composition, resulting in very stiff and more fragile materials.

The comparison of crystallization and mechanical properties of i-PP samples containing mainly regiodefects and a monomodal and narrow distribution of molecular weights ($M_w/M_n \approx 2$) with those of a sample having similar microstructure and a bimodal distribution of molecular masses ($M_w/M_n \approx 15$) has indicated that the polymorphic behavior and the kinetics of crystallization of the latter sample are mainly regulated by the fractions of chains having higher molecular masses, whereas the presence of chains with lower molecular masses induces a slightly higher drawability. This result is in agreement with studies performed using the EXXPOL technology, which have shown that a tailored distribution of molecular masses obtained using metallocene catalysts may lead to i-PP products having properties fully competitive or even enhanced with respect to the properties of classic commercial i-PPs produced with Ziegler−Natta catalysts.[46]

Acknowledgment. Financial support from Basell Polyolefins, Ferrara (Italy), and from the "Ministero dell'Istruzione, dell'Università e della Ricerca" of Italy (PRIN 2004 project) is gratefully acknowledged. We thank Riccardo Frabetti for performing the polymerization experiments and Dr. Dieter Lilge for providing the SEC data. The X-ray diffraction experiments were carried out at Centro Interdipartimentale di Metodologie Chimico-Fisiche, University of Naples Federico II.

References and Notes

(1) De Rosa, C.; Auriemma, F.; Circelli, T.; Waymouth, R. M. *Macromolecules* **2002**, *35*, 3622.
(2) Auriemma, F.; De Rosa, C. *Macromolecules* **2002**, *35*, 9057.
(3) De Rosa, C.; Auriemma, F.; Circelli, T.; Longo, P.; Boccia, A. C. *Macromolecules* **2003**, *36*, 3465.
(4) Auriemma, F.; De Rosa, C.; Boscato, T.; Corradini, P. *Macromolecules* **2001**, *34*, 4815.

(5) De Rosa, C.; Auriemma, F.; Di Capua, A.; Resconi, L.; Guidotti, S.; Camurati, I.; Nifant'ev, I. E.; Laishevtsev, I. P. *J. Am. Chem. Soc.* **2004**, *126*, 17040.
(6) De Rosa, C.; Auriemma, F.; Perretta, C. *Macromolecules* **2004**, *37*, 6843.
(7) Resconi, L.; Cavallo, L.; Fait, A.; Piemontesi, F. *Chem. Rev.* **2000**, *100*, 1253.
(8) Spaleck, W.; Küber, F.; Winter, A.; Rohrmann, J.; Bachmann, B.; Antberg, M.; Dolle, V.; Paulus, E. *Organometallics* **1994**, *13*, 954.
(9) Resconi, L.; Piemontesi, F.; Camurati, I.; Sudmeijer, O.; Nifant'ev, I. E.; Ivchenko, P. V.; Kuz'mina, L. G. *J. Am. Chem. Soc.* **1998**, *120*, 2308.
(10) Resconi, L.; Balboni, D.; Baruzzi, G.; Fiori, C.; Guidotti, S.; Mercandelli, P.; Sironi, A. *Organometallics* **2000**, *19*, 420.
(11) Nifant'ev, I. E.; Guidotti, S.; Resconi, L.; Laishevtsev, I. (Basell: Italy) PCT Int. Appl. WO 01/47939, 2001.
(12) Resconi, L.; Guidotti, S.; Camurati, I.; Nifant'ev, I. E.; Laishevtsev, I. *Polym. Mater. Sci. Eng.* **2002**, *87*, 76.
(13) Fritze, C.; Resconi, L.; Schulte, J.; Guidotti, S. (Basell: Italy) PCT Int. Appl. WO 03/00706, 2003.
(14) Nifant'ev, I. E.; Laishevtsev, I. P.; Ivchenko, P. V.; Kashulin, I. A.; Guidotti, S.; Piemontesi, F.; Camurati, I.; Resconi, L.; Klusener, P. A. A.; Rijsemus, J. J. H.; de Kloe, K. P.; Korndorffer, F. M. *Macromol. Chem. Phys.* **2004**, *205*, 2275.
(15) Resconi, L.; Guidotti, S.; Camurati, I.; Frabetti, R.; Focante, F.; Nifant'ev, I. E.; Laishevtsev, I. P. *Macromol. Chem. Phys.* **2005**, *206*, 1405.
(16) Covezzi, M.; Fait, A. PCT Int. Appl. WO 01/44319, Basell, 2001.
(17) Moraglio, G.; Gianotti, G.; Bonicelli, U. *Eur. Polym. J.* **1973**, *9*, 693.
(18) Wunderlich, B. In *Macromolecular Physics*; Academic Press: New York, 1973; Vol. I, p 63. Bu, H. S.; Cheng, S. Z. D.; Wunderlich, B. *Makromol. Chem. Rapid. Commun.* **1988**, *9*, 75.
(19) (a) Mezghani, K.; Phillips, P. J. *Polymer* **1998**, *39*, 3735. (b) Mezghani, K.; Phillips, P. J. *Polymer* **1997**, *38*, 5725. (c) Mezghani, K.; Phillips, P. J. *Polymer* **1995**, *36*, 2407. (d) Mezghani, K.; Campbell, R. A.; Phillips, P. J. *Macromolecules* **1994**, *27*, 997. (e) Campbell, R. A.; Phillips, P. J.; Lin, J. S. *Polymer* **1993**, *34*, 4809.
(20) Bond, E. B.; Spruiell, J. E. *J. Polym. Sci., Part B: Polym. Phys.* **1999**, *37*, 3050.
(21) Natta, G.; Corradini, P. *Nuovo Cimento Suppl.* **1960**, *15*, 40.
(22) Fischer, D.; Mülhaupt, R. *Macromol. Chem. Phys.* **1994**, *195*, 1433.
(23) Thomann, R.; Wang, C.; Kressler, J.; Mülhaupt, R. *Macromolecules* **1996**, *29*, 8425.
(24) Alamo, R. G.; Kim, M. H.; Galante, M. J.; Isasi, J. R.; Mandelkern, L. *Macromolecules* **1999**, *32*, 4050.
(25) VanderHart, D. L.; Alamo, R. G.; Nyden, M. R.; Kim, M. H.; Mandelkern, L. *Macromolecules* **2000**, *33*, 6078.
(26) Alamo, R. G.; VanderHart, D. L.; Nyden, M. R.; Mandelkern, L. *Macromolecules* **2000**, *33*, 6094.
(27) Thomann, R.; Semke, H.; Maier, R. D.; Thomann, Y.; Scherble, J.; Mülhaupt, R.; Kressler, J. *Polymer* **2001**, *42*, 4597.
(28) De Rosa, C.; Auriemma, F.; Spera, C.; Talarico, G.; Tarallo, O. *Macromolecules* **2004**, *37*, 1441.
(29) Lotz, B.; Graff, S.; Wittmann, J. C. *J. Polym. Sci., Polym. Phys.* **1986**, *24*, 2017. Kojima, M. *J. Polym. Sci.* **1967**, *5*, 245. Kojima, M. *J. Polym. Sci.* **1968**, *A-2*, 1255. Morrow, D. R.; Newman, B. A. *J. Appl. Phys.* **1968**, *39*, 4944.
(30) Nyden, M. R.; VanderHart, D. L.; Alamo, R. G. *Comput. Theor. Polym. Sci.* **2001**, *11*, 175.
(31) Enikolopyan, N. S.; Akopyan, E. L.; Styrikovich, N. M.; Kechekyan, A. S.; Nikol'skii, V. G. *J. Polym. Sci., Part B: Polym. Phys.* **1987**, *25*, 1203.
(32) Lu, F.-M.; Spruiell, J. E. *J. Appl. Polym. Sci.* **1987**, *34*, 1521.
(33) Misra, S.; Lu, F.-M.; Spruiell, J. E.; Richeson, G. C. *J. Appl. Polym. Sci.* **1995**, *56*, 1761.
(34) Bond, E. B.; Spruiell, J. E. *J. Appl. Polym. Sci.* **2001**, *82*, 3223. Bond, E. B.; Spruiell, J. E. *J. Appl. Polym. Sci.* **2001**, *82*, 3237.
(35) De Rosa, C.; Auriemma, F.; Spera, C. *Macromol. Symp.* **2004**, *218*, 113.
(36) Paukkeri, R.; Lehtinen, A. *Polymer* **1993**, *34*, 4075.
(37) Galante, M. J.; Mandelkern, L.; Alamo, G. R.; Lehtinen, A.; Paukkeri, R. *J. Therm. Anal.* **1996**, *47*, 913.
(38) Gahleitner, M.; Bachner, C.; Ratajski, E.; Rohaczek, G.; Neibl, W. *J. Appl. Polym. Sci.* **1999**, *73*, 2507.
(39) Sanchez, I. C.; Eby, R. K. *J. Res. Natl. Bur. Stand., Sect. A* **1973**, *77*, 353.
(40) Sanchez, I. C.; Eby, R. K. *Macromolecules* **1975**, *8*, 638.
(41) Flory, P. J. *Trans. Faraday Soc.* **1955**, *51*, 848.
(42) Fischer, E. W.; Sterzel, H. J.; Wegner, G. *Kolloid Z. Z. Polym.* **1973**, *251*, 980.
(43) Sanchez, I. C.; Colson, J. P.; Eby, R. K. *J. Appl. Phys.* **1973**, *44*, 4332. Sanchez, I. C.; Peterlin, A.; Eby, R. K.; McCrakin, F. L. *J. Appl. Phys.* **1974**, *45*, 4216.
(44) Eby, R. K. *J. Appl. Phys.* **1966**, *34*, 2442.
(45) Bolz, L. H.; Eby, R. K. *J. Res. Natl. Bur. Stand.* **1965**, *69A*, 481.
(46) Speca, A. N.; McAlpin, J. J. In *Metallocene-Catalyzed Polymers: Materials, Properties, Processing and Market*; Benedikt, G. M., Goodall, B. L., Eds.; Plastic Design Library: New York, 1998; p 73. Mehta, A. K.; Chen, M. C.; McAlpin, J. J. In *Metallocene-Catalyzed Polymers: Materials, Properties, Processing and Market*; Benedikt, G. M., Goodall, B. L., Eds.; Plastic Design Library: New York, 1998; p 261.

MA051004X